Molecular and Cellular Endocrinology 427 (2016) 143–154

Contents lists available at ScienceDirect

Molecular and Cellular Endocrinology

journal homepage: www.elsevier.com/locate/mce

Targeted inactivation of the mouse epididymal beta-defensin 41 alters sperm flagellar beat pattern and zona pellucida binding

Ida Björkgren [a, b, 1], Luis Alvarez [c], Nelli Blank [d], Melanie Balbach [d], Heikki Turunen [a, b], Teemu Daniel Laajala [e, f], Jussi Toivanen [a], Anton Krutskikh [g], Niklas Wahlberg [h], Ilpo Huhtaniemi [g], Matti Poutanen [a, i], Dagmar Wachten [d], Petra Sipilä [a, *]

[a] Department of Physiology and Turku Center for Disease Modeling, Institute of Biomedicine, University of Turku, Turku, Finland
[b] Turku Doctoral Programme of Biomedical Sciences, Turku, Finland
[c] Center of Advanced European Studies and Research (Caesar), Department of Molecular Sensory Systems, Bonn, Germany
[d] Center of Advanced European Studies and Research (Caesar), Minerva Research Group Molecular Physiology, Bonn, Germany
[e] Department of Mathematics and Statistics, University of Turku, Turku, Finland
[f] Institute for Molecular Medicine Finland (FIMM), University of Helsinki, Helsinki, Finland
[g] Institute of Reproductive and Developmental Biology, Imperial College London, Hammersmith Campus, London, United Kingdom
[h] Department of Biology, Lund University, Lund, Sweden
[i] Institute of Medicine, Sahlgrenska Academy, University of Gothenburg, Gothenburg, Sweden

ARTICLE INFO

Article history:
Received 5 October 2015
Received in revised form
25 February 2016
Accepted 9 March 2016
Available online 14 March 2016

Keywords:
Beta-defensin
Epididymis
Sperm maturation
Flagellar motility pattern
Sperm-oocyte binding
iCre knock-in

ABSTRACT

During epididymal maturation, sperm acquire the ability to swim progressively by interacting with proteins secreted by the epididymal epithelium. Beta-defensin proteins, expressed in the epididymis, continue to regulate sperm motility during capacitation and hyperactivation in the female reproductive tract. We characterized the mouse beta-defensin 41 (DEFB41), by generating a mouse model with *iCre* recombinase inserted into the first exon of the gene. The homozygous *Defb41*$^{iCre/iCre}$ knock-in mice lacked *Defb41* expression and displayed iCre recombinase activity in the principal cells of the proximal epididymis. Heterozygous *Defb41*$^{iCre/+}$ mice can be used to generate epididymis specific conditional knock-out mouse models. Homozygous *Defb41*$^{iCre/iCre}$ sperm displayed a defect in sperm motility with the flagella primarily bending in the pro-hook conformation while capacitated wild-type sperm more often displayed the anti-hook conformation. This led to a reduced straight line motility of *Defb41*$^{iCre/iCre}$ sperm and weaker binding to the oocyte. Thus, DEFB41 is required for proper sperm maturation.
© 2016 Elsevier Ireland Ltd. All rights reserved.

1. Introduction

After leaving the testis, immature sperm travel through the different epididymal segments, the initial segment, caput, corpus and cauda, where proteins secreted by the epithelial cells interact with and modify the sperm plasma-membrane. During this transit, the sperm mature and acquire the ability to swim progressively, although they are kept in an immotile state until ejaculation (Robaire et al., 2000; Cornwall, 2009; Yanagimachi, 1994). In passage through the most proximal segments, the sperm tail is stabilized, allowing the straight-line movement that is necessary to localize the oocyte (Yeung et al., 1992, 1993; Jeulin et al., 1996). In addition, the sperm membrane is modified to promote capacitation in the female reproductive tract (Visconti et al., 1995; Lewis and Aitken, 2001). Throughout the epididymal transit, sperm are protected from autoimmunity and potentially harmful bacteria by antimicrobial proteins secreted by the epididymal epithelium (Cobellis et al., 2010; Yenugu et al., 2004; Lin et al., 2008; Yu et al., 2013).

Beta-defensins form a protein family involved in both sperm maturation and antimicrobial defense (Klüver et al., 2006; Selsted and Ouellette, 2005; Klotman and Chang, 2006; Yenugu et al., 2004; Zhou et al., 2004; Tollner et al., 2004; Lin et al., 2008; Zhao

Abbreviations: Defb, Beta-defensing; KI, Knock-in; AR, Androgen receptor; IVF, *In vitro* fertilization; PKA, Protein kinase A; SACY, Soluble adenylyl cyclase; ZP, Zona pellucida.

* Corresponding author. Department of Physiology, Institute of Biomedicine, University of Turku, Kiinamyllynkatu 10, FI-20520, Turku, Finland.
E-mail address: petra.sipila@utu.fi (P. Sipilä).
[1] Present address: Department of Molecular and Cell Biology, UC Berkeley, Berkeley, CA, USA.

http://dx.doi.org/10.1016/j.mce.2016.03.013
0303-7207/© 2016 Elsevier Ireland Ltd. All rights reserved.

et al., 2011; Yu et al., 2013). A majority of the currently known beta-defensin genes (39 genes in humans, 43 in rats and 52 in mice) are evolutionarily conserved in mammals, where they form four to five syntenic gene clusters (Patil et al., 2005; Schutte et al., 2002). Beta-defensins are mainly expressed in the epithelial cells of the male reproductive tract, especially in testis and in the different segments of the epididymis (Patil et al., 2005). Two beta-defensins have been shown to have antimicrobial functions *in vivo*; deletion of mouse beta-defensin1 lead to delayed bacterial clearance from the lung (Moser et al., 2002) or higher number of bacteria in the bladder (Morrison et al., 2002), whereas overexpression of the mouse beta-defensin *Spag11a* (also known as BIN1b), showed an effect on epididymal infection resistance (Fei et al., 2012). However, despite the antimicrobial function of beta-defensins, concurrent deletion of nine beta-defensins, expressed in the reproductive tract, did not cause inflammation under normal animal housing conditions (Zhou et al., 2013). In contrast, several studies have shown a role for beta-defensins in sperm maturation, especially regulating sperm motility. In rats, the beta-defensins DEFB15 and SPAG11b bind to the sperm head and contribute to the maintenance and acquisition of sperm motility, respectively (Zhou et al., 2004; Zhao et al., 2011). Knock-down of either of the two genes led to reduced motility of caput sperm (Zhou et al., 2004; Zhao et al., 2011). In the case of SPAG11b, this was attributed to a reduced uptake of Ca^{2+} during epididymal transit (Zhou et al., 2004). Similarly the knock-out of a cluster of nine mouse beta-defensins caused altered Ca^{2+} signaling in epididymal sperm, which led to premature capacitation and acrosome reaction (Zhou et al., 2013). DEFB22/DEFB126 is secreted from corpus epididymis and binds to the sperm membrane, forming the most exterior part of the glycocalyx (Yudin et al 2003, 2008). The macaque DEFB126 is required for sperm to penetrate the cervical mucus (Tollner et al., 2008) and, interestingly, a common deletion in human DEFB126 hinders sperm from penetrating the mucus, thereby reducing pregnancy rates (Tollner et al., 2011). In addition, release of DEFB126 from the sperm membrane during capacitation is required for oocyte fertilization (Tollner et al., 2004).

To further clarify the role of beta-defensins in sperm maturation, we have studied the role of mouse *Defb41*, which is expressed in the most proximal part of the epididymis (Jalkanen et al., 2005). *Defb41* is located on chromosome 1qA4 and, like most beta-defensins consists of two short exons, which are 113 bp and 353 bp in size. The 62 amino acid long gene product contains a putative signal sequence, which is cleaved between amino acids 21 and 22 to produce the mature 41 amino acid DEFB41 protein. Further, DEFB41 contains six highly conserved cysteines typical for beta-defensins (Jalkanen et al., 2005). Similar to several other epididymal beta-defensins, *Defb41* is regulated by androgens. The expression of *Defb41* begins between day 8 and 13 after birth and increases until adulthood, due to the rise in testosterone levels during puberty (Jalkanen et al., 2005; Hamil et al., 2000; Liu et al., 2001; Ibrahim et al., 2001; Palladino et al., 2003). The mouse *Defb41* is orthologous to the human and macaque *DEFB110*, which both have 69% identity to the mouse protein (human Gene ID: 245913/Ensembl: ENSG00000203970; macaque Gene ID: 707363/Ensembl: ENSMMUG00000029616), however, no studies on gene function have been performed for these species.

In light of the previous studies on beta-defensins, and because of the segment-specific expression of *Defb41* in the initial segment (IS) and caput (CAP) of the mouse epididymis, we hypothesized that the protein has a function in sperm maturation. Thus, we generated a *Defb41* knock-in (KI) mouse model in which the cDNA coding for codon improved *Cre* recombinase (*iCre*, codon usage optimized for mammals (Shimshek et al., 2002)) is inserted into the translation start site of the *Defb41* locus. Homozygous $Defb41^{iCre/iCre}$ mice show deletion of both *Defb41* alleles, while the heterozygous $Defb41^{iCre/+}$ mice can be used to generate conditional knock-out models through the specific expression of *iCre* in the principal cells of the epididymal epithelium and the consequent deletion of floxed alleles.

2. Materials and methods

2.1. Ethic statement

Mice were housed in individually ventilated cages under controlled conditions of light (12 h light/12 h dark), temperature (21 ± 3 °C), and humidity (55% ± 15%). The mice were given soy-free natural-ingredient feed (RM3 (E), Special Diets Services), tap water *ad libitum*, and were housed in specific pathogen-free conditions at the Central Animal Laboratory, University of Turku, complying with international guidelines on the care and use of laboratory animals. All animal handling was conducted in accordance with the Finnish Animal Ethics Committee license, and the institutional animal care policies, which fully meet the requirements of European Union Directive 2010/63/EU and European Convention for the protection of vertebrate animals used for experimental and other scientific purposes (ETS No. 123, appendix A).

2.2. Generation of the Defb41 iCre KI mouse line

For cloning the *Defb41 iCre* KI targeting construct, the BAC clone containing the *Defb41* locus was purchased from RZPD German Resource Center for Genome Research (ImaGenes GmbH). The first exon of *Defb41* together with the two homology arms (1700 bp and 7951 bp long) were subcloned into the pACYC177 minimal backbone vector using Red/ET recombination technology (Angrand et al., 1999). An *iCre*-neomycin phosphotransferase (neo^r) expression cassette was inserted into the translation initiation site of the *Defb41* gene. Mutated FRT sites were located around the $iCre\text{-}neo^r$ cassette to allow recombinase mediated cassette exchange if needed (Fig. 1A). All primer sequences used in cloning are available on request.

The targeting construct was electroporated into AB2.2 embryonic stem (ES) cells, (129/Sv/Ev background, Lexicon Genetics). The clones were screened for homologous recombination by PCR over the 1700 bp 5'-homology arm using the Expand Long Template PCR System (Roche). The primers used for screening were DefbScrF1: CGGTATGAAATAGTGCTCTGAACTT and DefbScrR1: ATTCTCCTTTCTGATTCTCCTCATC (Fig. 1A). The correct targeting was further confirmed by PCR over the 7951 bp 3'-homology arm using the following primers, Defb41 3′ Fw: TCAAACAAGACCCCGTACAA and Defb41 e2 Re: TGTGTGCATGGATGGAGATT. The PCR was carried out using LongAmp Taq DNA Polymerase according to the manufacturer's instruction (New England BioLabs). Finally, the PCR products were sequenced to ascertain correct recombination. Chimeric mice were generated by injecting a correctly targeted ES cell clone into C57BL/6N blastocysts. Chimeric males were bred with wild type (wt) C57BL/6N females to obtain heterozygous $Defb41^{iCre/+}$ mice. Heterozygous hybrid males were backcrossed to C57Bl/6N for three generations and then bred with each other to obtain homozygous, *Defb41*-deficient, *iCre* KI mice, referred to as $Defb41^{iCre/iCre}$ mice in the text. $Defb41^{iCre/iCre}$ mice were genotyped as previously described (Björkgren et al., 2012). For the experiments the control wild type $Defb41^{+/+}$ mice and the $Defb41^{iCre/+}$ and $Defb41^{iCre/iCre}$ mice were all obtained from the same litters.

The histology of the $Defb41^{iCre/iCre}$ mouse epididymis was determined by dissecting the epididymides of $Defb41^{+/+}$ and $Defb41^{iCre/iCre}$ male mice at different ages, from two-months to seven-months of age. The tissue was fixed overnight in 4% paraformaldehyde (PFA) and embedded in paraffin. Hematoxylin and

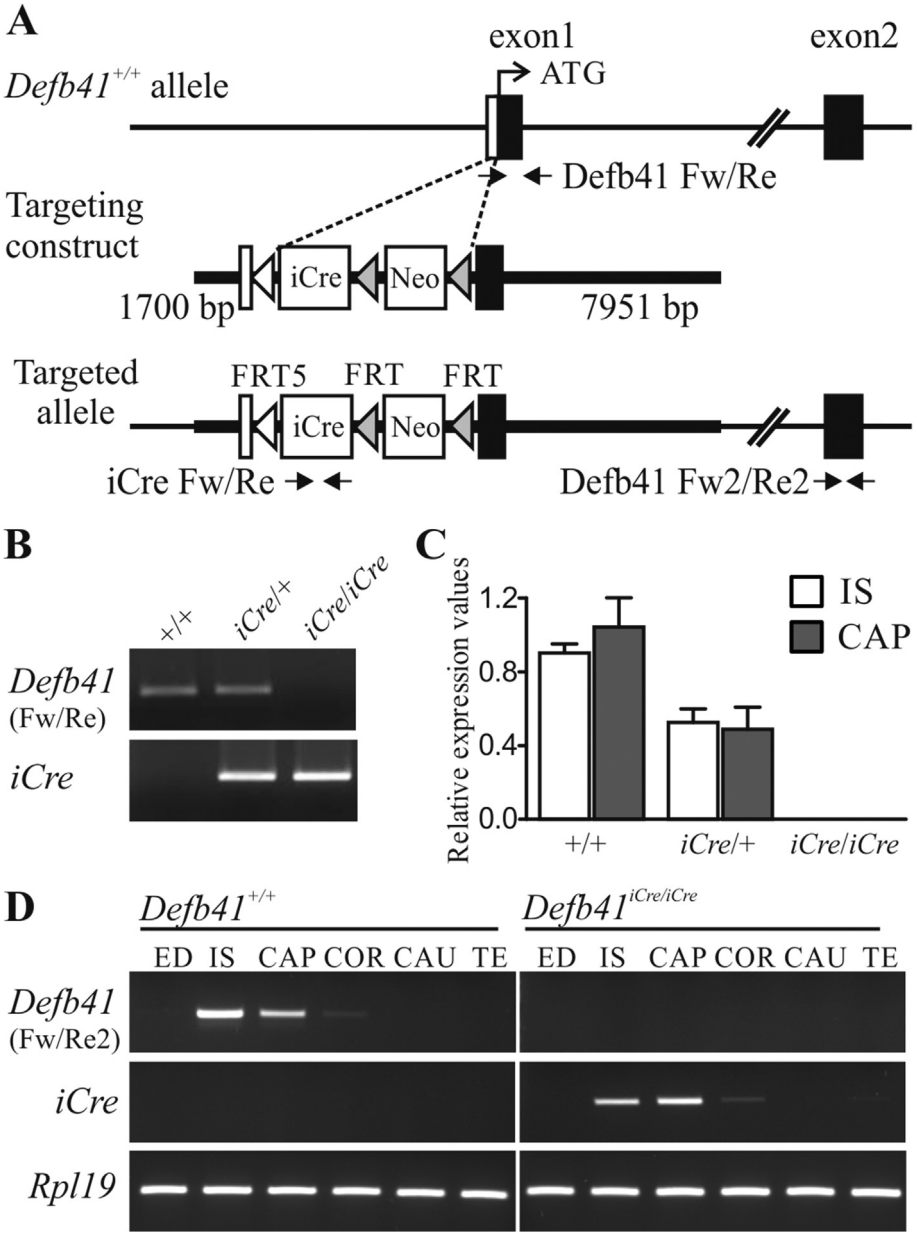

Fig. 1. The Defb41 iCre knock-in construct and detection of Defb41 deletion. (A) Construct used for gene targeting in ES cells and structure of the targeted allele. (B) Genomic PCR of two-month-old mice epididymides showing absence of Defb41 exon 1 and presence of iCre DNA in the *Defb41*$^{iCre/iCre}$ mice. (C) Quantitative RT-PCR analysis of Defb41 exon 2 expression in the initial segment (IS) and caput (CAP) of two-month-old mice (n = 3). Expression levels presented as mean (±SEM), relative to *Rpl19* and *Pgk1* expression. (D) RT-PCR analyses of *Defb41* and *iCre* expression in testis (TE), efferent ducts (ED) and the different epididymal segments of two-month-old *Defb41*$^{+/+}$ and *Defb41*$^{iCre/iCre}$ mice. Defb41 and iCre primer pair locations are shown in (A). The expression level of *Rpl19* was used as a control. COR, corpus; CAU, cauda.

eosin (HE) staining was performed by standard procedures.

2.3. RNA isolation and RT-PCR

To analyze the expression pattern of *iCre* and *Defb41*, two-month-old *Defb41*$^{+/+}$, *Defb41*$^{iCre/+}$, and *Defb41*$^{iCre/iCre}$ male mice were euthanized and various tissues and different segments of the epididymis were dissected and snap frozen. To analyze the Cre expression of heterozygous *Defb41*$^{iCre/+}$; CAG$^{Cre/+}$ mice, the IS and CAP of mice used in the sperm binding assay were similarly isolated. For time-point expression studies, the whole epididymis of 7-, 14-, 17-, 20-, 25-, 30- and 40-day-old *Defb41*$^{iCre/iCre}$ mice was dissected (each age n = 3). Total RNA was isolated from the tissues using TRIsure according to the manufacturer's instructions (Bioline). For generation of cDNA, 1 μg of total RNA was treated with deoxyribonuclease I (DNaseI, Amplification Grade, Invitrogen) and reverse-transcribed using the DyNAmo cDNA synthesis kit (Thermo Scientific). To detect *Defb41* and *iCre* expression, the RT-reaction was performed using Biotools DNA Polymerase (10.002) according to the manufacturer's instructions. The cDNA was diluted 1:50–1:100 for qRT-PCR analyses of *Cre*, *iCre*, and *Defb41* exon 2, expression. Quantitative PCR was performed using the DyNAmo SYBR Green qPCR Kit (Thermo Scientific). All samples and standards were run in triplicates. Ribosomal protein L19 (*Rpl19*) and phosphoglycerate kinase 1 (*Pgk1*) were used as endogenous controls to equalize for the amounts of RNA in the different tissues. Primers for

Defb41 detection were Fw: TCC ATT GCC TTT TCT TGT CC and Re2: TGT GTG CAT GGA TGG AGA TT, Tm 59 °C and primers for *Defb41* exon 2 detection were Re2, as previously, and Fw2: AGA TGT GAA AAA GTG CGA GGA, Tm 59 °C. The sequence and qRT-PCR conditions of the *Rpl19*, *Pgk1*, *Cre* and *iCre* primers were previously described (Turunen et al., 2012; Björkgren et al., 2012, 2014; Sakai and Miyazaki, 1997).

2.4. Analyzing epididymal iCre recombinase activity utilizing $Ar^{loxP/Y}$; $Defb41^{iCre/iCre}$ mice

For analyzing the activity of iCre in the different cell types of the epididymal epithelium, $Defb41^{iCre/iCre}$ mice were crossed with the previously described Androgen receptor (AR)-floxed mouse line (De Gendt et al., 2004). $AR^{loxP/Y}$; $Defb41^{iCre/iCre}$ mice were euthanized at the age of 35 days and the epididymides were fixed overnight with 4% paraformaldehyde, embedded in paraffin and prepared for histological analyses according to standard procedures. For double labeling of AR and the different epithelial cell types of the epididymis, the sections were incubated with the following antibodies overnight at 4 °C: rabbit anti-AR N-20 (1:1000 dilution, sc-816, Santa Cruz Biotechnology), goat polyclonal anti-forkhead box I1 for clear and narrow cells (1:100 dilution, ab20454, AbCam), and mouse monoclonal anti-Cytokeratin 5/6 for basal cells (1:100 dilution, M723729, Dako). The primary antibodies were diluted in PBS supplemented with 1% bovine serum albumin (BSA). The antibody–antigen complexes were visualized by incubation for 30 min at room temperature with, for AR detection; Alexa Fluor 488-conjugated rat anti-rabbit antibodies, and for detection of the cell-type specific antigens; Alexa Fluor 594-conjugated rat anti-goat or anti-mouse (1:200 dilution, Invitrogen). All samples were counterstained with 4′,6-diamino-2-phenylindole dihydrochloride (DAPI, Sigma) and mounted in Mowiol 4–88 (Sigma).

2.5. In vivo fertility

The breeding performance of six $Defb41^{iCre/iCre}$ male mice was followed in normal mating conditions. Two-month-old males were mated with wt C57Bl/6N female mice and the number of litters and offspring of each male was recorded during a time period of six months. Values were compared to those obtained from $Defb41^{+/+}$ male mice in breeding, at the same time and in the same animal room.

2.6. In vitro fertilization

In vitro fertilization (IVF) was conducted using two-month-old male mice. Sperm from six $Defb41^{+/+}$, six $Defb41^{iCre/+}$, and five $Defb41^{iCre/iCre}$ mice were collected during four experimental days, using at least one animal of each genotype per day. Cauda was dissected out and two small incisions were made to allow sperm to swim out into HTF medium containing BSA (K-RVFE-50, William A. Cook Australia Pty. Ltd) for 15 min at 37°, 89% N_2/6% CO_2/5% O_2, after which sperm were counted using a Bürker hemozytometer chamber (Hawksley). IVF was performed using 50,000 spermatozoa of each male, incubated in 200 μl HTF medium, together with oocytes in cumulus oophorus collected from 2 to 3 euthanized, superovulated FVB/N females. After 6 h incubation, the zygotes were washed through three drops of HTF and incubated further overnight. The number of fertilized oocytes was determined the following day as the percentage of oocytes/sample that were fertilized and cleaved to two-cell-stage embryos. The mean ± SD were then calculated from the results of the total mice used in each study group.

For competitive IVF sperm from four $Defb41^{iCre/iCre}$ mice, age from two to four months, and five age matched $Defb41^{+/+}$ control males were collected as described above. 20,000 spermatozoa from one $Defb41^{iCre/iCre}$ and one $Defb41^{+/+}$ male were combined into one sample which was put in to two separate fertilization dishes in 200 μl HTF medium. Oocytes in cumulus oophorus from 2 superovulated FVB/N females was added to each fertilization dish as described above. After 6 h incubation, the zygotes were washed through three drops of HTF and then cultured o/n. After reaching 2-cell stage the embryos were moved into KSOM + AA-medium containing BSA, (Millipore) and cultured further until blastocyst stage. Blastocysts were collected and subjected to lysis as described previously (Scavizzi et al., 2015) and genotyped using the same primers and PCR conditions that were used to genotype $Defb41^{iCre/iCre}$ mice (Björkgren et al., 2012) except that in the PCR reaction mix 5 ul of lysate was used and the number of PCR cycles was 50. The mean ± SD were then calculated for both genotypes, $Defb41^{+/+}$ and $Defb41^{iCre/+}$, from the total number of blastocysts obtained from the competitive IVF.

2.7. Sperm-zona pellucida binding

Next the effect of the loss of DEFB41 on sperm-zona pellucida binding efficiency was analyzed. In addition, to ensure that the effects seen are not caused by Cre toxicity, a CAG-Cre mouse line, where Cre is under the cytomegalovirus immediate early enhancer-chicken beta-actin hybrid (CAG) promoter, was utilized (Sakai and Miyazaki, 1997) in the sperm-zona pellucida binding assay. $CAG^{Cre/+}$ mice were mated with $Defb41^{iCre/iCre}$ mice to produce mice heterozygous for both *Cre* and *iCre* ($Defb41^{iCre/+}$; $CAG^{Cre/+}$), and thus having higher total Cre recombinase protein levels than in either mouse line alone. Sperm from two to three month-old wild type control (wt, no genetic modifications), $Defb41^{iCre/+}$, $Defb41^{iCre/iCre}$, $CAG^{Cre/+}$ and double heterozygous $Defb41^{iCre/+}$; $CAG^{Cre/+}$ males (n = 3–6), were collected in KSOM + AA-medium for 15 min at 37 °C, 89% N2/6% CO2/5% O2. The oocytes were collected from superovulated FVB/N females and cumulus oophorus was removed by hyaluronidase (0.6 mg/ml, Specialty Media) treatment. 40,000 spermatozoa from each male were incubated with 15–30 zona pellucida intact oocytes for 1 h at 37 °C, 89% N_2/6% CO_2/5% O_2 in 30 μl of KSOM-medium. After co-incubation, the gametes were washed three times with fresh KSOM medium to remove loosely attached spermatozoa, and fixed briefly in 4% PFA. From each male, spermatozoa bound to ten, randomly chosen oocytes were counted under the microscope by assessing the number of sperm in one focal plane.

2.8. Sperm capacitation

Analyses of sperm capacitation were performed according to the method previously described (Wertheimer et al., 2008). Briefly, caudal sperm from two-month-old $Defb41^{+/+}$, $Defb41^{iCre/+}$, and $Defb41^{iCre/iCre}$ mice (n = 5) were collected in modified non-capacitating Whitten-HEPES medium (Platt et al., 2009), pH 7.3, for 15 min at 37 °C. Each sperm sample was divided into five aliquots to which 20 mM $NaHCO_3$ and 10 mg/ml BSA were added. Sperm aliquots were collected after 0, 30, 60, 90, and 120 min incubation and the proteins were extracted by boiling in Laemmli sample buffer (Laemmli, 1970). Protein tyrosine phosphorylation was used as a read-out for sperm capacitation. Phosphorylation was assessed by Western blotting using a monoclonal anti-phosphotyrosine antibody (1:5000 dilution; Millipore) as primary antibody followed by a peroxidase-conjugated anti-mouse secondary antibody (1:5000 dilution; GE Healthcare). The detected levels of tyrosine phosphorylation were normalized to the expression level of alpha-tubulin. The membrane was stripped by

incubation with 6 M Guanidine HCl, 10% Triton X-100, 20 mM Tris–HCl, 0.1 M beta-mercaptoethanol, pH 7.5 twice for 5 min at room temperature. Thereafter, the membrane was blocked and re-hybridized with tubulin-alpha ab-2 antibody (1:5000 dilution; Lab Vision). The stained proteins were quantified from digital images using the ImageJ software.

2.9. Sperm acrosome reaction

2.9.1. Isolation of mouse zone pellucida

To induce the acrosome reaction with solubilized zonae pellucidae, female mice were superovulated by intraperitoneal injection of 10 I.U. hCG (human Chorionic Gonadotropin; Intergonan, SimposiumVet) 3 days before the experiment. 14 h before oocyte preparation, mice were injected with 10 I.U. PMSG (Pregnant Mare's Serum Gonadotropin; Ovogest, SimposiumVet). Cumulus-enclosed oocytes were prepared from the oviducts in TYH buffer (138 mM NaCl, 4.8 mM KCl, 2 mM $CaCl_2$, 1.2 mM KH_2PO_4, 1 mM $MgSO_4$, 5.6 mM glucose, 0.5 mM sodium pyruvate, 10 mM L-lactate, pH 7.4.) containing 300 μg/ml hyaluronidase (Sigma). After 15 min, cumulus-free oocytes were transferred into fresh buffer and washed twice. Zona pellucidae and oocytes were separated by shear forces generated by expulsion from 50 nm pasteur pipettes. Zona pellucidae were counted and transferred into fresh buffer.

2.9.2. Analysis of acrosomal exocytosis

For analysis of acrosomal exocytosis, caudal sperm from two-month-old *Defb41*$^{+/+}$, and *Defb41*$^{iCre/iCre}$ mice (each genotype n = 3) were collected and 100 μl $1 \cdot 10^6$ sperm (TYH buffer, 3 mg/ml BSA) were capacitated with 25 mM $NaHCO_3$ for 90 min at 37 °C. As a control, sperm were incubated in BSA buffer only (non-capacitated). Acrosome reaction was induced by incubating sperm with 50 heat-solubilized mouse zona pellucida or 2 μM ionomycin for 10 min at 37 °C. As vehicle control, sperm were incubated in 1% DMSO. The sperm suspension was spun down, the supernatant was discarded, and the sperm were resuspended in 100 μl PBS buffer. Samples were air dried on microscope slides and fixed for 30 min in 100% ethanol at room temperature. Sperm were labeled with 5 μg/ml PNA-FITC (L7381, Sigma–Aldrich) and 2 μg/ml DAPI for 30 min in the dark. For each condition, at least 600 cells were analyzed using ImageJ. Acrosome-reacted sperm were counted and normalized to non-capacitated sperm.

2.10. Intracellular PKA/SACY and cAMP levels

To analyze the expression level of protein kinase A (PKA) and soluble adenylyl cyclase (SACY) by Western blot, total lysates were isolated from *Defb41*$^{+/+}$ testis and *Defb41*$^{+/+}$ and *Defb41*$^{iCre/iCre}$ sperm and processed as previously described (Krahling et al., 2013). The following primary antibodies were used: PKA [Cα], (1:4000 dilution, 610980, BD Transduction Laboratories), sAC R21, (1:1000 dilution, (Zippin et al., 2003)). Primary antibodies were detected with fluorescently-labeled secondary antibodies (anti-mouse IRDye680LT and anti-mouse IRDye800CW, 1:20,000 dilution, LI-COR Biosciences) and analyzed using the LI-COR Odyssey system.

For cAMP measurements, sperm were isolated by incision of the cauda epididymidis in modified TYH-medium containing 138 mM NaCl, 4.8 mM KCl, 2 mM $CaCl_2$, 1.2 mM KH_2PO_4, 1 mM $MgSO_4$, 5.6 mM glucose, 0.5 mM sodium pyruvate, 10 mM L-lactate, pH 7.4, supplemented with 3 mg/ml BSA. After 15 min swim out at 37 °C and 5% CO_2, sperm were counted. Basal cAMP levels as well as the increase in cAMP levels in the presence of 25 mM $NaHCO_3$ and/or 0.75 mM IBMX was determined using the CatchPoint cAMP Fluorescent Assay Kit (Molecular Devices). The assay was performed according to the protocol provided with the kit.

2.11. Sperm motility analyses

For motility analyses, the sperm were collected as described above. Flagellar movements and the different motility parameters were analyzed under non-capacitating and capacitating conditions as previously described (Krahling et al., 2013), with the exception of using smaller moving windows (0.5 s side) to quantify the different parameters. To quantify the flagellar movement, a portion of the flagellum (arc length distance of 50 μm from the head) was followed. The angle φ(t) between the long axis of symmetry of the cell and a line crossing the middle flagellar portion and the sperm head described a periodic movement. The flagellar beat asymmetry index corresponded to the average angle (<φ>) within the 0.5 s side moving window. The flagellar amplitude was calculated by fitting a sinusoidal time trace to the angle around its mean (φ(t) - (<φ>). The average flagellar beat asymmetry index, amplitude and frequency were calculated from all frames in the recording (between 400 and 4000 frames). Between 4 and 14 sperm were analyzed in non-capacitating and capacitating conditions for each animal (four *Defb41*$^{+/+}$ and five *Defb41*$^{iCre/iCre}$ animals). To assess if the sperm flagellum moved in both pro- and anti-hook conformations and to detect the average angle of each conformation, 120 frames (approximately 5 full beat cycles) depicting pro- and anti-hook motility were quantified separately. Four sperm from each animal were analyzed under non-capacitating and capacitating conditions (three *Defb41*$^{+/+}$ and three *Defb41*$^{iCre/iCre}$ animals). For quantification of the sperm motility path, 4–16 films were recorded for each animal (three *Defb41*$^{+/+}$ and three *Defb41*$^{iCre/iCre}$ mice), containing data from a total number of 60–200 sperm cells.

2.12. Sequence alignment and phylogenetic analysis

To reveal which epididymal beta-defensin family members are most similar to DEFB41, amino acid sequences of 23 family members (and different isoforms of SPAG11B) expressed in the mouse caput epididymidis were acquired along with rat and human orthologs from the NCBI database (total of 60 sequences, Supplemental Table S1). The amino acid sequences were then aligned using the T-COFFEE algorithm (Notredame et al., 2000) utilizing the BLOSUM matrix during the alignment procedure (Supplemental Fig. S1). The aligned sequences were imported into MEGA6 (Tamura et al., 2013) and analyzed using Maximum likelihood. Uniform rates were assumed across sites and the JTT-model of amino acid evolution was used. To evaluate the robustness of the phylogenetic hypothesis, bootstrapping was used with 500 replications.

2.13. Statistical analyses

For sperm cAMP measurements and motility analyses, statistical comparisons were carried out using Students *t*-test. For statistical analyses of organ weights, sperm count and animal fertility, One-way ANOVA and for sperm flagellar movement Mann–Whitney test in the GraphPad Prism 5 software (GraphPad Software, Inc.) was used. Statistical analyses for iCre expression at different age points and sperm – oocyte binding SigmaPlot 13.0 software was used. For iCre expression at different age points One-way ANOVA was performed and in the case of statistically significant results a pair-wise multiple comparisons with Holm-Sidak method was used. For sperm – oocyte binding Kruskal–Wallis one-way analysis was performed, and in the case of statistically significant results, Dunn's test was used for pair-wise multiple comparisons. $p \leq 0.05$ was assigned as the limit of statistical significance.

To test each of the seven sperm motility parameters separately (VCL, curvilinear velocity; VAP, average path velocity; VSL, straight

linear velocity; LHD, lateral head displacement; Wobble, LIN, linearity; and STR, straightness), statistical analyses were performed using a mixed-effects model:

$$y = b_0 + b_1 \cdot K + b_2 \cdot C + b_3 \cdot K \cdot C + u_{0,i} + e_{i,f} \quad (1)$$

The model Eq. (1) shows the effect of *Defb41* ablation and/or capacitation on sperm motility and takes into account animal specific variation and the difference in number of films recorded for each animal. Motility data from 4 to 16 films per animal was recorded, and the average motility of the detected sperm was calculated for each of the films (response y). Non-motile sperm with VAP <20 μm/s were excluded from the calculations. The model terms K and C were used as binary indicators for knock-out or capacitation, respectively. Model term K adopted the value zero for *Defb41*$^{+/+}$ sperm and one for *Defb41*$^{iCre/iCre}$ and the term C adopted the value zero for non-capacitated and one for capacitated sperm. The fixed effect terms $b_0 - b_3$ indicated population effects specific for the baseline level (b_0, confirms a motility baseline above zero by comparing non-capacitated *Defb41*$^{+/+}$ sperm motility to zero), mere *Defb41* knockout effect (b_1, non-capacitated *Defb41*$^{+/+}$ versus *Defb41*$^{iCre/iCre}$ sperm motility), mere capacitation effect (b_2, capacitated versus non-capacitated *Defb41*$^{+/+}$ sperm motility), and the interaction of the 2 × 2 factorial design (b_3, if *Defb41*$^{iCre/iCre}$ sperm respond differently to capacitation than *Defb41*$^{+/+}$ sperm). Calculated average values and statistical significance for the fixed effect terms b_0–b_3 are presented in Supplemental Table S2. The random effect u_0 captured animal-specific variation (n = 3 *Defb41*$^{+/+}$, n = 3 *Defb41*$^{iCre/iCre}$) and was assumed to be normally distributed. By introducing u_0 we compensated for the different numbers of films that were recorded for each animal. Finally, the normally distributed model error term e captured the remaining data noise over the individual animals (index i) and recorded films (index f). The model was fitted using the statistical software R (http://www.R-project.org) and its package lme4 (http://CRAN.R-project.org/package=lme4).

3. Results

3.1. Generation of the Defb41 iCre KI mouse line

To inactivate the *Defb41* gene in mice, the *iCre* recombinase expression cassette was targeted into the first exon of the gene (Fig. 1A). Thereby, *iCre* was expressed under the control of the regulatory region of *Defb41* while the expression of functional *Defb41* was abolished. After insertion of the targeting vector into ES cells, PCR and sequencing of the 5'- and 3'-homology arms confirmed correct targeting (the sequencing data is available on request). Mice were generated by injection of ES cells into blastocysts and their genotypes were confirmed by PCR (Fig. 1B). Expression of *iCre* and lack of *Defb41* exon 1 and 2 expression in the epididymis of *Defb41*$^{iCre/iCre}$ mice was confirmed by RT-PCR and qRT-PCR, respectively (Fig. 1C,D). The single wild-type allele of *Defb41*$^{iCre/+}$ mice gave rise to half the amount of exon 2 mRNA products when compared to *Defb41*$^{+/+}$ mice (relative expression of *Defb41*$^{+/+}$ IS: 0,9 ± 0,1, CAP 1,0 ± 0,3; *Defb41*$^{iCre/+}$ IS: 0,5 ± 0,1, CAP: 0,5 ± 0,2). No expression was detected in *Defb41*$^{iCre/iCre}$ mice IS or CAP. Epididymis and testis weight of two-month-old *Defb41*$^{iCre/+}$ and *Defb41*$^{iCre/iCre}$ mice was similar to *Defb41*$^{+/+}$ mice (Relative weight of epididymis mg/whole body weight g: *Defb41*$^{+/+}$, 1.13 ± 40.1; *Defb41*$^{iCre/+}$, 1.06 ± 0.1; *Defb41*$^{iCre/iCre}$, 1.08 ± 0.1, relative testis weight: *Defb41*$^{+/+}$ 3.25 ± 0.5; *Defb41*$^{iCre/+}$, 3.20 ± 0.3; *Defb41*$^{iCre/iCre}$, 3.07 ± 0.6). Further, HE staining of tissue sections showed similar histology in *Defb41*$^{+/+}$ and *Defb41*$^{iCre/iCre}$ mice in all the age groups studied (Supplemental Fig. S2).

3.2. Localization of the Defb41 locus expression driving iCre recombinase

The expression of *Defb41* in the mouse epididymis has been previously defined (Jalkanen et al., 2005). To analyze whether the expression pattern was similar for the *iCre* recombinase under the *Defb41* regulatory region, we performed qRT-PCR studies. The results indicated *iCre* expression in the most proximal segments of the epididymis, with highest expression in the IS (Supplemental Fig. S3A). The expression level in CAP was a third of the expression level in IS and only one animal out of three showed marginal expression in the spleen and testis (Supplemental Fig. S3A). However, we could not detect any recombinase activity in the testis and spleen. The onset of *iCre* expression in the epididymis takes place between 7 and 14 days after birth, and the expression reaches peak level at 25 days postpartum. A slight decline in expression can be observed in 30 and 40 days of age (Supplemental Fig. S3B). To define the epithelial cell types expressing *iCre* under the *Defb41* locus, we used mice with a floxed *Ar* (De Gendt et al., 2004). Immunohistochemical analysis revealed that all epithelial cells in the epididymis of *Defb41*$^{iCre/iCre}$ mice expressed AR (Supplemental Fig. S3C, D). *AR*$^{loxP/Y}$; *Defb41*$^{iCre/iCre}$ mice lacked AR expression in the principal cells of the IS and CAP, while the basal and narrow/clear cells still displayed AR expression (Supplemental Fig. S3C, D). Thus, the *iCre* recombinase is specifically expressed in the principal cells of the proximal epididymis under the control of the *Defb41* promoter.

3.3. Fertility analyses

Defb41$^{iCre/iCre}$ males were fertile and showed no difference in litter number and litter sizes compared to *Defb41*$^{+/+}$ males (*Defb41*$^{+/+}$, 6.6 ± 2.5 pups/litter; *Defb41*$^{iCre/iCre}$, 6.7 ± 2.3 pups/litter) within the time period analyzed, from 2 months of age until 8 months of age. *In vitro* fertilization experiments confirmed this result, as *Defb41*$^{+/+}$, *Defb41*$^{iCre/+}$, and *Defb41*$^{iCre/iCre}$ mice sperm fertilized similar numbers of oocytes (Fig. 2A). In addition, in competitive IVF from a total of 129 blastocysts obtained, 63 (mean 15.8 ± 6.3) were fertilized by wild type Defb41^{+} sperm and 62 (mean 15.5 ± 4.8) by Defb41^{iCre} sperm, thus showing equal fertilizing capacity of the two mouse lines. Furthermore, we analyzed the ability of the *Defb41*$^{+/+}$ and *Defb41*$^{iCre/iCre}$ sperm to undergo the acrosome reaction. However, there was no difference in the number of acrosome reacted sperm between *Defb41*$^{+/+}$ and *Defb41*$^{iCre/iCre}$ mice when utilizing a calcium ionophore or ZP proteins as inducers (Fig. 2B). In addition, both sperm morphology (Fig. 2C–E) and sperm count were similar between *Defb41*$^{+/+}$, *Defb41*$^{iCre/+}$, and *Defb41*$^{iCre/iCre}$ mice (sperm count in mil.: *Defb41*$^{+/+}$, 7.2 ± 3.3; *Defb41*$^{iCre/+}$, 8.0 ± 7.0; *Defb41*$^{iCre/iCre}$, 9.0 ± 3.8).

In contrast, there was a significant decline in the ability of *Defb41*$^{iCre/iCre}$ sperm to bind to the oocyte as compared to sperm from wt and *Defb41*$^{iCre/+}$ mice (Fig. 3B). To show that the sperm-ZP binding phenotype is not caused by Cre toxicity rather than reduced DEFB41 levels, we performed a binding assay with the transgenic CAG$^{Cre/+}$ mouse line with ubiquitous *Cre* expression throughout the epididymis (Sakai and Miyazaki, 1997). CAG$^{Cre/+}$ mice express *Cre* at similar levels compared to heterozygous *Defb41*$^{iCre/+}$ mice whereas double heterozygous *Defb41*$^{iCre/+}$; CAG$^{Cre/+}$ mice produce similar levels of total *Cre* expression compared to *Defb41*$^{iCre/iCre}$ mice (Fig. 3A). However, the binding efficiency of CAG$^{Cre/+}$ sperm was indistinguishable from wt sperm and *Defb41*$^{iCre/+}$; CAG$^{Cre/+}$ mice sperm was comparable to that of *Defb41*$^{iCre/+}$ mice sperm and significantly higher than that of *Defb41*$^{iCre/iCre}$ mice ($p < 0.001$, Fig. 3B). Thus, the level of *Defb41* expression was critical for the binding efficiency. In contrast, the level of *Cre* expression did

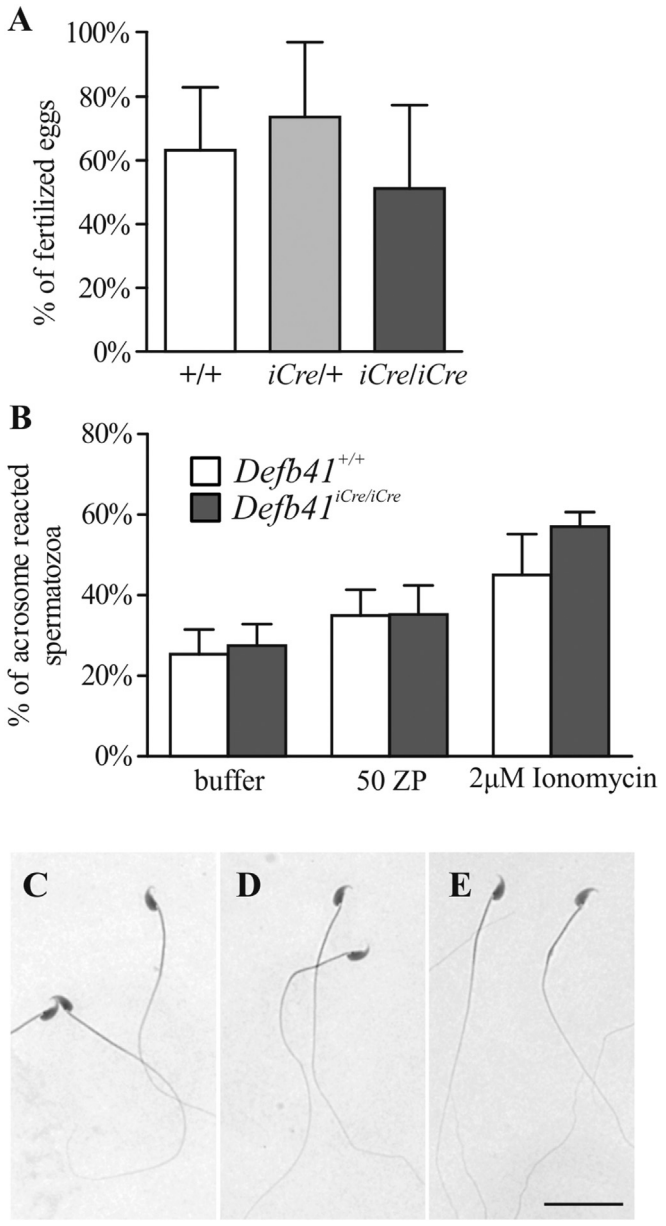

Fig. 2. Sperm fertility analyses of two-month-old males. (A) In vitro fertilization of *Defb41*$^{+/+}$ (n = 6), *Defb41*$^{iCre/+}$ (n = 6) and *Defb41*$^{iCre/iCre}$ (n = 5) males. Data represents mean (±SD) percentage of fertilized oocytes. (B) Analysis of the acrosome reaction (each genotype n = 3) presented as mean (±SD) percentage of acrosome reacted spermatozoa after incubation with buffer alone, mouse zona pellucida (ZP) or Ionomycin. The morphology of sperm collected from (C) *Defb41*$^{+/+}$, (D) *Defb41*$^{iCre/+}$, and (E) *Defb41*$^{iCre/iCre}$ mice cauda. Scale bar 25 µm.

not affect the sperm binding capability.

3.4. Sperm motility

To analyze whether the lack of *Defb41* affects sperm motility, we studied the flagellar beat and motility of *Defb41*$^{+/+}$ and *Defb41*$^{iCre/iCre}$ sperm. We first analyzed the flagellar beat of tethered sperm. The analyses showed a significant difference in symmetry of flagellar bending between *Defb41*$^{+/+}$ and *Defb41*$^{iCre/iCre}$ sperm. Under non-capacitating conditions, *Defb41*$^{+/+}$ and *Defb41*$^{iCre/iCre}$ sperm were beating symmetrically (Fig. 4A, D). Capacitation resulted in a more asymmetric flagellar beat with the tail alternatively bending in a prominent pro-hook (Fig. 4B, E) and anti-hook (Fig. 4C, F) conformation. For non-capacitated *Defb41*$^{+/+}$ and *Defb41*$^{iCre/iCre}$ sperm, the average flagellar bending was biased towards an anti-hook conformation as indicated by a positive asymmetry index (Fig. 4G). However, after capacitation, the flagellum of *Defb41*$^{iCre/iCre}$ sperm was bending more often than *Defb41*$^{+/+}$ in the pro-hook conformation, as indicated by a more negative asymmetry index compared to *Defb41*$^{+/+}$ sperm (Fig. 4G). To analyze this difference in detail, we studied the two flagellar conformations separately. However, the bending angle of the *Defb41*$^{iCre/iCre}$ sperm tail in the pro- and anti-hook conformation was similar to *Defb41*$^{+/+}$ sperm (Fig. 4H). Thus, *Defb41*$^{iCre/iCre}$ sperm were able to bend in both the pro- and anti-hook conformation; however, they seemed to bend more often in the pro-hook conformation compared to *Defb41*$^{+/+}$ sperm. We also analyzed the amplitude and frequency of the flagellar beat, but there was no difference between *Defb41*$^{iCre/iCre}$ and *Defb41*$^{+/+}$ mouse sperm under non-capacitating and capacitating conditions (Fig. 4I, J).

To investigate whether the difference in flagellar bending affected the motility pattern of freely swimming sperm, we analyzed the swimming path of *Defb41*$^{+/+}$ and *Defb41*$^{iCre/iCre}$ sperm. Whereas there was no difference between *Defb41*$^{+/+}$ and *Defb41*$^{iCre/iCre}$ under non-capacitating conditions, *Defb41*$^{iCre/iCre}$ sperm showed a significant decrease in straight line velocity (VSL) after capacitation compared to *Defb41*$^{+/+}$ sperm ($p = 0.037$, Fig. 5A, Supplemental Table S2). Consequently, sperm linear motility (LIN, calculated as VSL:VCL) and the straightness of sperm movements (STR, calculated as VSL:VAP) were also significantly decreased (LIN: $p = 0.00034$, Fig. 5B; STR: $p = 0.0005$, Fig. 5C, Supplemental Table S2). Taken together, our results indicate that *Defb41*$^{iCre/iCre}$ sperm swim in more curved paths after capacitation, and consequently, show lower progressive motility compared to the sperm of *Defb41*$^{+/+}$ mice.

Flagellar beat frequency and, thereby, sperm motility crucially rely on PKA-dependent phosphorylation of proteins in the axoneme, activated by an increase in the intracellular cAMP concentration through the atypical adenylyl cyclase SACY (Esposito et al., 2004; Wandernoth et al., 2010). Thus, we investigated whether changes in the cAMP signaling-cascade underlie the motility defects observed in *Defb41*$^{iCre/iCre}$ sperm. Protein expression of SACY and PKA did not differ between *Defb41*$^{+/+}$ and *Defb41*$^{iCre/iCre}$ mice (Fig. 6A). Furthermore, neither basal cAMP levels nor cAMP levels after activation of SACY by bicarbonate were different between genotypes (Fig. 6B). Downstream of PKA, protein tyrosine phosphorylation occurs, which is considered a hallmark of capacitation (Visconti et al., 1995). Since *Defb41*$^{iCre/iCre}$ sperm displayed a defect in flagellar bending after capacitation, we analyzed tyrosine phosphorylation in *Defb41*$^{+/+}$, *Defb41*$^{iCre/+}$, and *Defb41*$^{iCre/iCre}$ sperm. However, there was no difference between genotypes (Fig. 6C, D).

3.5. Phylogenetic analysis of beta-defensins expressed in the caput epididymidis

The highest amino acid sequence similarity to DEFB41 was found from its human and rat orthologs, DEFB110 and DEFB17, respectively (Supplemental Fig. S4). Similar close clustering of known beta-defensin orthologs was observed in the analyses. DEFB41 formed a clade with DEFB18, which is also physically close to *Defb41* in chromosome 1 (Supplemental Fig. S4).

4. Discussion

Sperm maturation in the epididymis depends on the segment specific expression and secretion of proteins from the epididymal

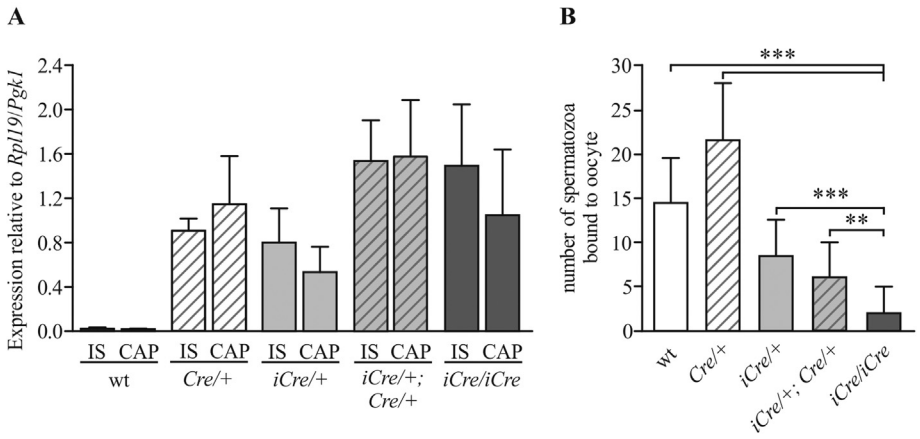

Fig. 3. Sperm oocyte binding and Cre toxicity assessment. (A) Total Cre expression levels in wild type (wt, n = 2), Defb41$^{iCre/+}$ (n = 3), Defb41$^{iCre/iCre}$ (n = 4), CAG$^{Cre/+}$ (n = 3) and double heterozygous Defb41$^{iCre/+}$;CAG$^{Cre/+}$ (n = 3) animals. Expression levels presented as mean (±SD). (B) Mean (±SD) number of sperm bound to the oocyte in the sperm − ZP binding assay (n = 3–6). Statistical significance is calculated using the Kruskal–Wallis one-way test, *, $p \leq 0.05$; **, $p \leq 0.01$; ***, $p \leq 0.001$.

epithelium (Robaire et al., 2000; Cornwall, 2009). The beta-defensin family is of particular interest, as the proteins have been shown to interact with sperm after release into the epididymal lumen (Zhou et al., 2004; Zhao et al., 2011; Yudin et al., 2003, 2008) and thereby promote fertility by regulating sperm motility (Zhou et al., 2004; Zhao et al., 2011; Yu et al., 2013). To further clarify the role of the beta-defensin family in sperm maturation, we generated a knock-out for *Defb41*, which is specifically expressed in the most proximal part of the juvenile and adult mouse epididymis (Jalkanen et al., 2005).

Defb41$^{iCre/iCre}$ male mice showed normal epididymal morphology and fertility. The rate of spermatogenesis did not differ between *Defb41*$^{+/+}$ and *Defb41*$^{iCre/iCre}$ mice as indicated by comparable numbers and morphology of spermatozoa. However, similar to other published beta-defensin models (Zhou et al., 2004; Zhao et al., 2011), sperm from *Defb41*$^{iCre/iCre}$ mice showed changes in motility. After capacitation, the flagellum of *Defb41*$^{iCre/iCre}$ sperm resided longer in the pro-hook conformation compared to *Defb41*$^{+/+}$ sperm. In addition, linearity and straightness of *Defb41*$^{iCre/iCre}$ sperm velocity was reduced after capacitation. Thus, the change in flagellar bending seemed to result in a different motility pattern. Although the different motility pattern was detected after capacitation, there was no discernable change in *Defb41*$^{iCre/iCre}$ sperm capacitation or acrosome reaction. The signaling pathways leading up to these events were not altered, as indicated by similar levels of PKA and protein tyrosine phosphorylation between control and *Defb41*$^{iCre/iCre}$ sperm.

Sperm motility and sperm-oocyte interaction are controlled by Ca^{2+} (Darszon et al., 2011). It has been suggested that hyperactive motility of sperm in the female reproductive tract is caused by an increased pH, which triggers influx of Ca^{2+} through CatSper channels (Kirichok et al., 2006). This increase in Ca^{2+} causes sperm to bend predominantly in a pro-hook formation. At the same time, there is a release of Ca^{2+} from inner stores that is thought to promote anti-hook bending (Marquez et al., 2007; Alasmari et al., 2013). Sperm from *CatSper* knock-out mice lack hyperactivated motility and are infertile (Ren et al., 2001; Quill et al., 2003; Jin et al., 2007; Qi et al., 2007), as they cannot penetrate the zona pellucida (Suarez et al., 1991, 1992; Ren et al., 2001; Quill et al., 2003). However, if the zona pellucida is removed from the oocyte, *CatSper* knock-out sperm are still able to fertilize the oocyte (Ren et al., 2001). Previous beta-defensin mouse models have shown a motility phenotype due to changes in Ca^{2+} signaling (Zhou et al., 2004, 2013). Beta-defensins are cationic molecules, which insert into phospholipid membranes forming holes or channels (Hall et al., 2007). Thereby, they possess anti-microbial properties but also, as in the case of SPAG11b, the ability to form or activate Ca^{2+} channels in the sperm membrane (Zhou et al., 2004). Lack of *Spag11b* in the rat epididymis led to reduced sperm motility, while the introduction of the protein to immature sperm gave rise to increased Ca^{2+} uptake and progressive motility (Zhou et al., 2004). On the contrary, the partial deletion of the mouse chromosome 8 beta-defensin cluster resulted in increased Ca^{2+}-uptake with premature hyperactivation and spontaneous acrosome reaction of the spermatozoa (Zhou et al., 2013). It was suggested that one or several of the beta-defensins in this study had a role in regulating CatSper or other calcium channels (Zhou et al., 2013). Thus, binding of beta-defensins to sperm in the epididymis could protect sperm from premature activation by inhibiting the activation of Ca^{2+} channels. In the case of *Defb41*, the predominant pro-hook formation of the sperm flagellum would indicate a role in regulating Ca^{2+}-signaling, possibly by direct or indirect inhibition of CatSper channels. Interestingly, sperm motility and VSL has been positively correlated with sperm-oocyte binding efficiency (Mahony et al., 2000; Yogev et al., 2000). Although the *Defb41*$^{iCre/iCre}$ sperm are produced in normal amounts and would capacitate and acrosome react, the more prominent pro-hook movements could lead to a reduced number of spermatozoa with the appropriate pattern of flagellar movement to bind to the oocyte. Few studies have analyzed the role of beta-defensins in sperm-oocyte interaction. It was shown that removal of DEFB126 from sperm promotes binding to the oocyte, while the deletion of chromosome 8 beta-defensins caused reduced amounts of bound sperm (Tollner et al., 2004; Zhou et al., 2013). The role of sperm binding affinity in fertilization is debatable as it has been shown that penetration of the oocyte can take place directly after the acrosome reacted sperm encounter zona pellucida (Jin et al., 2011). This could also explain why we did not observe a change in *Defb41*$^{iCre/iCre}$ fertility. If the acrosome reaction took place prior to oocyte contact, the reduced binding efficiency would not have had a significant effect on animal fertility *in vitro* or *in vivo*.

The beta-defensin family is a large family of proteins and the function of one particular beta-defensin is most likely compensated by other family members. This has also been observed in previous studies of beta-defensin knockout-mice (Morrison et al., 2002; Moser et al., 2002). In addition to *Defb41*, there are 22 beta-defensing expressed in the mouse caput epididymidis (Hu et al., 2014) and redundancy could explain the mild phenotype of

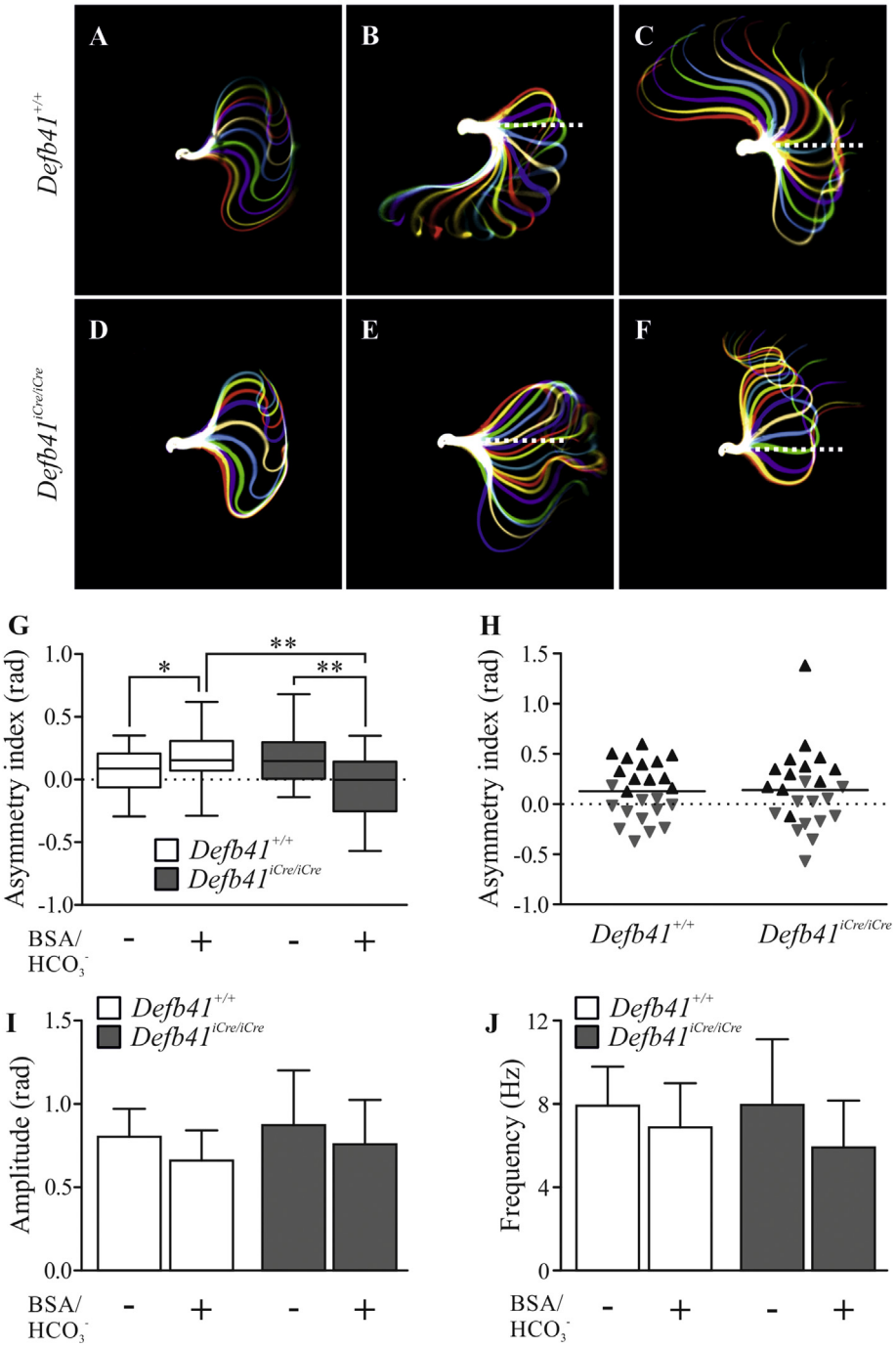

Fig. 4. Sperm flagellar movement. Representative image of the flagellar waveform of tethered, non-capacitated (A) *Defb41*$^{+/+}$ and (D) *Defb41*$^{iCre/iCre}$ sperm. Capacitated *Defb41*$^{+/+}$ and *Defb41*$^{iCre/iCre}$ sperm in (B, E) pro-hook and (C, F) anti-hook conformation. (G) Asymmetry index of flagellar bending (radian) in sperm from 3 to 5 *Defb41*$^{+/+}$ and *Defb41*$^{iCre/iCre}$ mice before (−) and after (+) induction of capacitation with BSA/HCO3-. Negative values indicate pro-hook and positive values anti-hook conformation. Data presented as median (±SD). Statistical significance is calculated using the Mann–Whitney test, *, $p \leq 0.05$; **, $p \leq 0.01$; ***, $p \leq 0.001$. (H) Separate analysis of the anti- and pro-hook conformations in capacitated *Defb41*$^{+/+}$ and *Defb41*$^{iCre/iCre}$ sperm. Each sperm is represented by a downward pointing triangle (showing average pro-hook angle) and an upward pointing triangle (the average anti-hook angle). Bar shows mean of total asymmetry index. (I) Mean (±SD) amplitude (radian) and (J) frequency (Hz) of the sperm flagellar beat in *Defb41*$^{+/+}$ and *Defb41*$^{iCre/iCre}$ mice (n = 3–5 mice).

Defb41$^{iCre/iCre}$ mice. Beta-defensin family members have low sequence similarity among the members suggesting that the molecular diversity of beta-defensins have evolved as a response to a range of diverse pathogens (Semple and Dorin, 2012). However, DEFB41 along with other beta-defensins share a 6-cysteine motif necessary for the disulfide bonding pattern; Cys1-Cys5, Cys2-Cys4, Cys3-Cys6, necessary for secondary structure typical for beta-defensins (Klüver et al., 2006). Phylogenetic analyses performed in our study are consistent with the previous observation that closest sequence similarity is found between family members that are physically close to each other in one genomic cluster (Morrison et al., 2003). The closest family member to mouse *Defb41* seems to be *Defb18* located next to *Defb41* in the chromosome 1. Interestingly, those beta-defensins whose lack has been shown to have

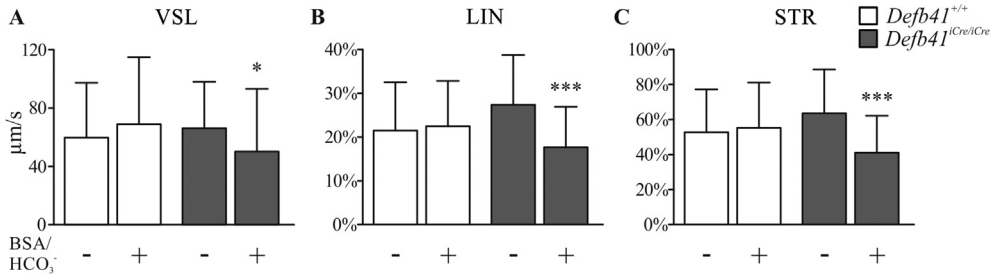

Fig. 5. Sperm motility. (A) Mean (±SD) straight line velocity (VSL), (B) linearity (LIN), and (C) straightness (STR) before (−) and after (+) induction of capacitation with BSA/HCO3- of freely swimming sperm from three *Defb41*$^{+/+}$ and *Defb41*$^{iCre/iCre}$ animals. Statistical significance, indicating difference in response to capacitation between *Defb41*$^{+/+}$ and *Defb41*$^{iCre/iCre}$ sperm, was calculated using a mixed effects model. *, $p \leq 0.05$, ***, $p \leq 0.001$.

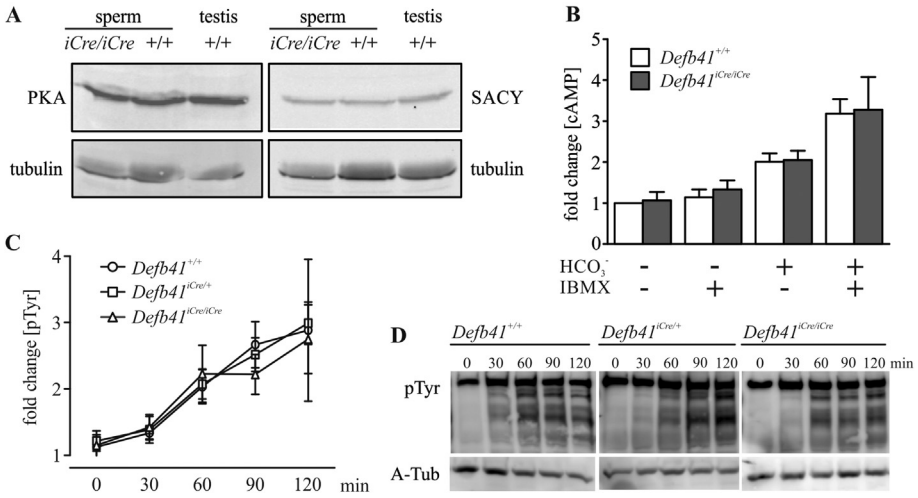

Fig. 6. Sperm capacitation and PKA signaling. (A) Western blot analysis of PKA and SACY expression levels in sperm and testis of *Defb41*$^{+/+}$ and *Defb41*$^{iCre/iCre}$ mice. (B) Mean (±SD) cAMP levels of sperm in HCO3- and/or IBMX. (C) Change in levels of tyrosine phosphorylation in *Defb41*$^{+/+}$, *Defb41*$^{iCre/+}$, and *Defb41*$^{iCre/iCre}$ sperm, 0–120 min after induction of capacitation. Levels of protein tyrosine phosphorylation are normalized to alpha-tubulin expression. The graph shows mean values (±SD) of five *Defb41*$^{+/+}$, *Defb41*$^{iCre/+}$, and *Defb41*$^{iCre/iCre}$ animals. (D) Representative Western blots demonstrating the increase in protein tyrosine phosphorylation (pTyr) observed after incubation in capacitating conditions. A-Tub, alpha-tubulin.

clear effects on fertility have an extended tail region with potential O-linked glycosylation sites after the last two core cysteines (Semple and Dorin, 2012). However, it is not clear how this difference in structure affects the functions of beta-defensins and further studies are required to resolve this question.

5. Conclusion

Our study shows a role for the novel mouse beta-defensin, *Defb41*, in sperm motility. By utilizing advanced measurement techniques detecting sperm flagellar motility, *Defb41*$^{iCre/iCre}$ sperm was shown to have an inverse flagellar beat pattern after capacitation. While ablation of *Defb41* expression does not give rise to morphological changes in the epididymis or spermatozoa, the change in flagellar movement results in an altered velocity of sperm motility as well as a reduction in oocyte binding. The function of DEFB41, thus, correlates with the role of beta-defensins as regulators of sperm maturation and the results from current study are consistent with view that beta-defensins might regulate Ca2+-uptake in the sperm membrane.

Acknowledgments

This work was supported by grants from The Academy of Finland and Sigrid Jusélius Foundation. The *Defb41 iCre* KI mouse line was generated in collaboration with Turku Center for Disease Modeling, TCDM, Turku, Finland, (www.tcdm.fi), and the authors thank the TCDM personnel for skillful assistance in various stages of this study. We further thank Tero Aittokallio, Department of Mathematics and Statistics, University of Turku, for assistance in the statistical analyses and the Cell Imaging Core, Turku Centre for Biotechnology, for assistance in imaging of fluorescently labeled samples.

Appendix A. Supplementary data

Supplementary data related to this article can be found at http://dx.doi.org/10.1016/j.mce.2016.03.013.

References

Alasmari, W., Costello, S., Correia, J., Oxenham, S.K., Morris, J., Fernandes, L., Ramalho-Santos, J., Kirkman-Brown, J., Michelangeli, F., Publicover, S., Barratt, C.L., 2013. Ca2+ signals generated by CatSper and Ca2+ stores regulate different behaviors in human sperm. J. Biol. Chem. 288, 6248–6258.

Angrand, P.O., Daigle, N., van der Hoeven, F., Scholer, H.R., Stewart, A.F., 1999. Simplified generation of targeting constructs using ET recombination. Nucleic Acids Res. 27, e16.

Björkgren, I., Gylling, H., Turunen, H., Huhtaniemi, I., Strauss, L., Poutanen, M., Sipilä, P., 2014. Imbalanced lipid homeostasis in the conditional Dicer1 knockout mouse epididymis causes instability of the sperm membrane. FASEB J. 29, 433–442.

Björkgren, I., Saastamoinen, L., Krutskikh, A., Huhtaniemi, I., Poutanen, M., Sipilä, P.,

2012. Dicer1 ablation in the mouse epididymis causes dedifferentiation of the epithelium and imbalance in sex steroid signaling. PLoS One 7, e38457.
Cobellis, G., Ricci, G., Cacciola, G., Orlando, P., Petrosino, S., Cascio, M.G., Bisogno, T., De Petrocellis, L., Chioccarelli, T., Altucci, L., Fasano, S., Meccariello, R., Pierantoni, R., Ledent, C., Di Marzo, V., 2010. A gradient of 2-arachidonoylglycerol regulates mouse epididymal sperm cell start-up. Biol. Reprod. 82, 451–458.
Cornwall, G.A., 2009. New insights into epididymal biology and function. Hum. Reprod. Update 15, 213–227.
Darszon, A., Nishigaki, T., Beltran, C., Trevino, C.L., 2011. Calcium channels in the development, maturation, and function of spermatozoa. Physiol. Rev. 91, 1305–1355.
De Gendt, K., Swinnen, J.V., Saunders, P.T., Schoonjans, L., Dewerchin, M., Devos, A., Tan, K., Atanassova, N., Claessens, F., Lecureuil, C., Heyns, W., Carmeliet, P., Guillou, F., Sharpe, R.M., Verhoeven, G., 2004. A Sertoli cell-selective knockout of the androgen receptor causes spermatogenic arrest in meiosis. Proc. Natl. Acad. Sci. U. S. A. 101, 1327–1332.
Esposito, G., Jaiswal, B.S., Xie, F., Krajnc-Franken, M.A., Robben, T.J., Strik, A.M., Kuil, C., Philipsen, R.L., van Duin, M., Conti, M., Gossen, J.A., 2004. Mice deficient for soluble adenylyl cyclase are infertile because of a severe sperm-motility defect. Proc. Natl. Acad. Sci. U. S. A. 101, 2993–2998.
Fei, Z., Hu, S., Xiao, L., Zhou, J., Diao, H., Yu, H., Fang, S., Wang, Y., Wan, Y., Wang, W., He, Y., Wang, C., Xu, G., Wang, Z., Zhang, Y., Fei, J., 2012. mBin1b transgenic mice show enhanced resistance to epididymal infection by bacteria challenge. Genes Immun. 13, 445–451.
Hall, S.H., Yenugu, S., Radhakrishnan, Y., Avellar, M.C., Petrusz, P., French, F.S., 2007. Characterization and functions of beta defensins in the epididymis. Asian J. Androl. 9, 453–462.
Hamil, K.G., Sivashanmugam, P., Richardson, R.T., Grossman, G., Ruben, S.M., Mohler, J.L., Petrusz, P., O'Rand, M.G., French, F.S., Hall, S.H., 2000. HE2beta and HE2gamma, new members of an epididymis-specific family of androgen-regulated proteins in the human. Endocrinology 141, 1245–1253.
Hu, S.-G., Zou, M., Y, G.-X., Ma, W.-B., Zhu, Q.-L., Li, X.-Q., Chen, Z.-J., Sun, Y., 2014. Androgenic regulation of beta-defensins in the mouse epididymis. Reprod. Biol. Endocrinol. 12, 76.
Ibrahim, N.M., Young, L.G., Frohlich, O., 2001. Epididymal specificity and androgen regulation of rat EP2. Biol. Reprod. 65, 575–580.
Jalkanen, J., Huhtaniemi, I., Poutanen, M., 2005. Discovery and characterization of new epididymis-specific beta-defensins in mice. Biochim. Biophys. Acta 1730, 22–30.
Jeulin, C., Lewin, L.M., Chevrier, C., Schoevaert-Brossault, D., 1996. Changes in flagellar movement of rat spermatozoa along the length of the epididymis: manual and computer-aided image analysis. Cell Motil. Cytoskelet. 35, 147–161.
Jin, J., Jin, N., Zheng, H., Ro, S., Tafolla, D., Sanders, K.M., Yan, W., 2007. Catsper3 and Catsper4 are essential for sperm hyperactivated motility and male fertility in the mouse. Biol. Reprod. 77, 37–44.
Jin, M., Fujiwara, E., Kakiuchi, Y., Okabe, M., Satouh, Y., Baba, S.A., Chiba, K., Hirohashi, N., 2011. Most fertilizing mouse spermatozoa begin their acrosome reaction before contact with the zona pellucida during in vitro fertilization. Proc. Natl. Acad. Sci. U. S. A. 108, 4892–4896.
Kirichok, Y., Navarro, B., Clapham, D.E., 2006. Whole-cell patch-clamp measurements of spermatozoa reveal an alkaline-activated Ca2+ channel. Nature 439, 737–740.
Klotman, M.E., Chang, T.L., 2006. Defensins in innate antiviral immunity. Nat. Rev. Immunol. 6, 447–456.
Klüver, E., Adermann, K., Schulz, A., 2006. Synthesis and structure-activity relationship of beta-defensins, multi-functional peptides of the immune system. J. Pept. Sci. 12, 243–257.
Krahling, A.M., Alvarez, L., Debowski, K., Van, Q., Gunkel, M., Irsen, S., Al-Amoudi, A., Strunker, T., Kremmer, E., Krause, E., Voigt, I., Wortge, S., Waisman, A., Weyand, I., Seifert, R., Kaupp, U.B., Wachten, D., 2013. CRIS-a novel cAMP-binding protein controlling spermiogenesis and the development of flagellar bending. PLoS Genet. 9, e1003960.
Laemmli, U.K., 1970. Cleavage of structural proteins during the assembly of the head of bacteriophage T4. Nature 227, 680–685.
Lewis, B., Aitken, R.J., 2001. Impact of epididymal maturation on the tyrosine phosphorylation patterns exhibited by rat spermatozoa. Biol. Reprod. 64, 1545–1556.
Lin, Y.Q., Li, J.Y., Wang, H.Y., Liu, J., Zhang, C.L., Wang, W.T., Liu, J., Li, N., Jin, S.H., 2008. Cloning and identification of a novel sperm binding protein, HEL-75, with antibacterial activity and expressed in the human epididymis. Hum. Reprod. 23, 2086–2094.
Liu, Q., Hamil, K.G., Sivashanmugam, P., Grossman, G., Soundararajan, R., Rao, A.J., Richardson, R.T., Zhang, Y.L., O'Rand, M.G., Petrusz, P., French, F.S., Hall, S.H., 2001. Primate epididymis-specific proteins: characterization of ESC42, a novel protein containing a trefoil-like motif in monkey and human. Endocrinology 142, 4529–4539.
Mahony, M.C., Rice, K., Goldberg, E., Doncel, G., 2000. Baboon spermatozoa-zona pellucida binding assay. Contraception 61, 235–240.
Marquez, B., Ignotz, G., Suarez, S.S., 2007. Contributions of extracellular and intracellular Ca2+ to regulation of sperm motility: release of intracellular stores can hyperactivate CatSper1 and CatSper2 null sperm. Dev. Biol. 303, 214–221.
Morrison, G., Kilanowski, F., Davidson, D., Dorin, J., 2002. Characterization of the mouse beta defensin 1, Defb1, mutant mouse model. Infect. Immun. 70, 3053–3060.
Morrison, G.M., Semple, C.A., Kilanowski, F.M., Hill, R.E., Dorin, J.R., 2003. Signal sequence conservation and mature peptide divergence within subgroups of the murine beta-defensin gene family. Mol. Biol. Evol. 20, 460–470.
Moser, C., Weiner, D.J., Lysenko, E., Bals, R., Weiser, J.N., Wilson, J.M., 2002. beta-Defensin 1 contributes to pulmonary innate immunity in mice. Infect. Immun. 70, 3068–3072.
Notredame, C., Higgins, D.G., Heringa, J., 2000. T-Coffee: a novel method for fast and accurate multiple sequence alignment. J. Mol. Biol. 302, 205–217.
Palladino, M.A., Mallonga, T.A., Mishra, M.S., 2003. Messenger RNA (mRNA) expression for the antimicrobial peptides beta-defensin-1 and beta-defensin-2 in the male rat reproductive tract: beta-defensin-1 mRNA in initial segment and caput epididymis is regulated by androgens and not bacterial lipopolysaccharides. Biol. Reprod. 68, 509–515.
Patil, A.A., Cai, Y., Sang, Y., Blecha, F., Zhang, G., 2005. Cross-species analysis of the mammalian beta-defensin gene family: presence of syntenic gene clusters and preferential expression in the male reproductive tract. Physiol. Genomics 23, 5–17.
Platt, M.D., Salicioni, A.M., Hunt, D.F., Visconti, P.E., 2009. Use of differential isotopic labeling and mass spectrometry to analyze capacitation-associated changes in the phosphorylation status of mouse sperm proteins. J. Proteome Res. 8, 1431–1440.
Qi, H., Moran, M.M., Navarro, B., Chong, J.A., Krapivinsky, G., Krapivinsky, L., Kirichok, Y., Ramsey, I.S., Quill, T.A., Clapham, D.E., 2007. All four CatSper ion channel proteins are required for male fertility and sperm cell hyperactivated motility. Proc. Natl. Acad. Sci. U. S. A. 104, 1219–1223.
Quill, T.A., Sugden, S.A., Rossi, K.L., Doolittle, L.K., Hammer, R.E., Garbers, D.L., 2003. Hyperactivated sperm motility driven by CatSper2 is required for fertilization. Proc. Natl. Acad. Sci. U. S. A. 100, 14869–14874.
Ren, D., Navarro, B., Perez, G., Jackson, A.C., Hsu, S., Shi, Q., Tilly, J.L., Clapham, D.E., 2001. A sperm ion channel required for sperm motility and male fertility. Nature 413, 603–609.
Robaire, B., Syntin, P., Jervis, K., 2000. The coming of age of the epididymis. In: Jegou, B. (Ed.), Testis, Epididymis and Technologies in the Year 2000. Springer-Verlag, New York, pp. 229–262.
Sakai, K., Miyazaki, J., 1997. A transgenic mouse line that retains Cre recombinase activity in mature oocytes irrespective of the cre transgene transmission. Biochem. Biophys. Res. Commun. 237, 318–324.
Scavizzi, F., Ryder, E., Newman, S., Raspa, M., Gleeson, D., Wardle-Jones, H., Montoliu, L., Fernandez, A., Dessain, M.-L., Larrigaldie, V., Khorshidi, Z., Vuolteenaho, R., Soininen, R., André, P., Jacquot, S., Hong, Y., Hrabe de Angelis, M., Ramirez-Solis, R., Doe, B., 2015. Blastocyst genotyping for quality control of mouse mutant archives: an ethical and economical approach. Transgenic Res. 24, 921–927.
Schutte, B.C., Mitros, J.P., Bartlett, J.A., Walters, J.D., Jia, H.P., Welsh, M.J., Casavant, T.L., McCray, P.B., 2002. Discovery of five conserved beta -defensin gene clusters using a computational search strategy. Proc. Natl. Acad. Sci. U. S. A. 99, 2129–2133.
Selsted, M.E., Ouellette, A.J., 2005. Mammalian defensins in the antimicrobial immune response. Nat. Immunol. 6, 551–557.
Semple, F., Dorin, J.R., 2012. β-Defensins: multifunctional modulators of infection, inflammation and more. J. Innate Immun. 4, 337–348.
Shimshek, D.R., Kim, J., Hübner, M.R., Spergel, D.J., Buchholz, F., Casanova, E., Stewart, A.F., Seeburg, P.H., Sprengel, R., 2002. Codon-improved Cre recombinase (iCre) expression in the mouse. Genesis 32, 19–26.
Suarez, S.S., Dai, X.B., DeMott, R.P., Redfern, K., Mirando, M.A., 1992. Movement characteristics of boar sperm obtained from the oviduct or hyperactivated in vitro. J. Androl. 13, 75–80.
Suarez, S.S., Katz, D.F., Owen, D.H., Andrew, J.B., Powell, R.L., 1991. Evidence for the function of hyperactivated motility in sperm. Biol. Reprod. 44, 375–381.
Tamura, K., Stecher, G., Peterson, D., Filipski, A., Kumar, S., 2013. Mega6: molecular evolutionary genetics analysis version 6.0. Mol. Biol. Evol. 30, 2725–2729.
Tollner, T.L., Venners, S.A., Hollox, E.J., Yudin, A.I., Liu, X., Tang, G., Xing, H., Kays, R.J., Lau, T., Overstreet, J.W., Xu, X., Bevins, C.L., Cherr, G.N., 2011. A common mutation in the defensin DEFB126 causes impaired sperm function and subfertility. Sci. Transl. Med. 3, 92ra65.
Tollner, T.L., Yudin, A.I., Treece, C.A., Overstreet, J.W., Cherr, G.N., 2008. Macaque sperm coating protein DEFB126 facilitates sperm penetration of cervical mucus. Hum. Reprod. 23, 2523–2534.
Tollner, T.L., Yudin, A.I., Treece, C.A., Overstreet, J.W., Cherr, G.N., 2004. Macaque sperm release ESP13.2 and PSP94 during capacitation: the absence of ESP13.2 is linked to sperm-zona recognition and binding. Mol. Reprod. Dev. 69, 325–337.
Turunen, H.T., Sipilä, P., Krutskikh, A., Toivanen, J., Mankonen, H., Hämäläinen, V., Björkgren, I., Huhtaniemi, I., Poutanen, M., 2012. Loss of cysteine-rich secretory protein 4 (crisp4) leads to deficiency in sperm-zona pellucida interaction in mice. Biol. Reprod. 86, 1–8.
Visconti, P.E., Bailey, J.L., Moore, G.D., Pan, D., Olds-Clarke, P., Kopf, G.S., 1995. Capacitation of mouse spermatozoa. I. Correlation between the capacitation state and protein tyrosine phosphorylation. Development 121, 1129–1137.
Wandernoth, P.M., Raubuch, M., Mannowetz, N., Becker, H.M., Deitmer, J.W., Sly, W.S., Wennemuth, G., 2010. Role of carbonic anhydrase IV in the bicarbonate-mediated activation of murine and human sperm. PLoS One 5, e15061.
Wertheimer, E.V., Salicioni, A.M., Liu, W., Trevino, C.L., Chavez, J., Hernandez-Gonzalez, E.O., Darszon, A., Visconti, P.E., 2008. Chloride is essential for capacitation and for the capacitation-associated increase in tyrosine

phosphorylation. J. Biol. Chem. 283, 35539–35550.
Yanagimachi, R., 1994. Mammalian fertilization. In: Knobil, E., Neill, J. (Eds.), The Physiology of Reproduction. Raven Press, New York, pp. 189–317.
Yenugu, S., Hamil, K.G., Radhakrishnan, Y., French, F.S., Hall, S.H., 2004. The androgen-regulated epididymal sperm-binding protein, human beta-defensin 118 (DEFB118) (formerly ESC42), is an antimicrobial beta-defensin. Endocrinology 145, 3165–3173.
Yeung, C.H., Cooper, T.G., Oberpenning, F., Schulze, H., Nieschlag, E., 1993. Changes in movement characteristics of human spermatozoa along the length of the epididymis. Biol. Reprod. 49, 274–280.
Yeung, C.H., Oberländer, G., Cooper, T.G., 1992. Characterization of the motility of maturing rat spermatozoa by computer-aided objective measurement. J. Reprod. Fertil. 96, 427–441.
Yogev, L., Gamzu, R., Botchan, A., Hauser, R., Paz, G., Yavetz, H., 2000. Zona pellucida binding improvement effect of different sperm preparation techniques is not related to changes in sperm motility characterizations. Fertil. Steril. 73, 1120–1125.
Yu, H., Dong, J., Gu, Y., Liu, H., Xin, A., Shi, H., Sun, F., Zhang, Y., Lin, D., Diao, H., 2013. The novel human beta-defensin 114 regulates lipopolysaccharide (LPS)-mediated inflammation and protects sperm from motility loss. J. Biol. Chem. 288, 12270–12282.
Yudin, A.I., Tollner, T.L., Li, M.W., Treece, C.A., Overstreet, J.W., Cherr, G.N., 2003. ESP13.2, a member of the beta-defensin family, is a macaque sperm surface-coating protein involved in the capacitation process. Biol. Reprod. 69, 1118–1128.
Yudin, A.I., Tollner, T.L., Treece, C.A., Kays, R., Cherr, G.N., Overstreet, J.W., Bevins, C.L., 2008. Beta-defensin 22 is a major component of the mouse sperm glycocalyx. Reproduction 136, 753–765.
Zhao, Y., Diao, H., Ni, Z., Hu, S., Yu, H., Zhang, Y., 2011. The epididymis-specific antimicrobial peptide beta-defensin 15 is required for sperm motility and male fertility in the rat (Rattus norvegicus). Cell Mol. Life Sci. 68, 697–708.
Zhou, C.X., Zhang, Y.L., Xiao, L., Zheng, M., Leung, K.M., Chan, M.Y., Lo, P.S., Tsang, L.L., Wong, H.Y., Ho, L.S., Chung, Y.W., Chan, H.C., 2004. An epididymis-specific beta-defensin is important for the initiation of sperm maturation. Nat. Cell Biol. 6, 458–464.
Zhou, Y.S., Webb, S., Lettice, L., Tardif, S., Kilanowski, F., Tyrrell, C., Macpherson, H., Semple, F., Tennant, P., Baker, T., Hart, A., Devenney, P., Perry, P., Davey, T., Barran, P., Barratt, C.L., Dorin, J.R., 2013. Partial deletion of chromosome 8 beta-defensin cluster confers sperm dysfunction and infertility in male mice. PLoS Genet. 9, e1003826.
Zippin, J.H., Chen, Y., Nahirney, P., Kamenetsky, M., Wuttke, M.S., Fischman, D.A., Levin, L.R., Buck, J., 2003. Compartmentalization of bicarbonate-sensitive adenylyl cyclase in distinct signaling microdomains. FASEB J. 17, 82–84.